INTERNATIONAL JOURNAL FOR NUMERICAL METHODS IN FLUIDS
Int. J. Numer. Meth. Fluids 2003; **42**:581–606 (DOI: 10.1002/fld.527)

Reduced order state-space models from the pulse responses of a linearized CFD scheme

Ann L. Gaitonde and D. P. Jones*,†

Department of Aerospace Engineering, University of Bristol, University Walk, Bristol BS8 1TR, U.K.

SUMMARY

This paper describes a method for obtaining a time continuous reduced order model (ROM) from a system of time continuous linear differential equations. These equations are first put into a time discrete form using a finite difference approximation. The unit sample responses of the discrete system are calculated for each system input and these provide the Markov parameters of the system. An eigenvalue realization algorithm (ERA) is used to construct a discrete ROM. This ROM is then used to obtain a continuous ROM of the original continuous system. The focus of this paper is on the application of this method to the calculation of unsteady flows using the linearized Euler equations on moving meshes for aerofoils undergoing heave or linearized pitch motions. Applying a standard cell-centre spatial discretization and taking account of mesh movement a continuous system of differential equations is obtained which are continuous in time. These are put into discrete time form using an implicit finite difference approximation. Results are presented demonstrating the efficiency of the system reduction method for this system. Copyright © 2003 John Wiley & Sons, Ltd.

1. INTRODUCTION

Unsteady flows about flexible structures occur in many areas. The focus of the work described here is the stability and responses of fixed wing aircraft. Theoretical prediction of unsteady flows require models of both the fluid motion and the structure. This paper is concerned with modelling the fluid motion. It describes early results of an ongoing program of work. The objective is to develop an efficient computational fluid model which permits aeroelastic calculations to be performed at much lower cost than is possible with full non-linear methods (see for example References [1–5]) whilst retaining reasonable accuracy. The full non-linear methods which typically have many thousands of degrees of freedom are too computationally expensive for use in industry. This is due to the fact that many thousands of parameter variations must be investigated. For an extensive review of fluid motion modelling from classical methods through to recent developments see Dowell and Hall Reference [6].

A first step in achieving improved efficiency for aeroelastic applications has been the use of time-linearized schemes. Such schemes model an unsteady flow as the sum of a steady

* Correspondence to: D. P. Jones, Department of Aerospace Engineering, University of Bristol Queen's Building, University Walk, Bristol, BS8 1TR, U.K.
† E-mail: dorian.jones@bris.ac.uk

Received January 2002
Revised 16 October 2002

base flow and a small dynamic perturbation. Depending on the choice of steady base flow model it may be possible to include many physical phenomena, for example shock waves, 3D vorticity and separated flows. However due to the assumption of a small dynamic perturbation any dynamic changes to these features must be small.

The particular base flows of interest to this work are statically non-linear, but the overall method is dynamically linear and therefore limit cycle oscillations due to fluid non-linearity cannot be modelled. However LCOs caused by structural non-linearity can be calculated [7]. Schemes of this type do not contain a mechanism to allow changes in the flow structure during the unsteady calculation [8], so for example if a shock is not present in the mean flow it cannot arise during the dynamic calculation.

Here the base flow is calculated using the non-linear Euler equations. Calculating unsteady flows by processing a general input through the unsteady time-linearized Euler equations presents no significant advance on the full non-linear equations as the number of degrees of freedom is the same. However there are two strategies which utilize these equations to provide improved efficiency over full non-linear calculations and are therefore useful tools for aeroelastic/aeroservoelastic analyses.

The first approach (not used in this work) assumes all perturbations to be harmonic and has been the focus of many studies, particularly in the field of turbomachinery, see References [8–15]. This reduces the problem to a steady-state calculation for the perturbation at a given frequency. This frequency can be chosen to be the natural frequency of vibration in a linear aeroelastic model under static load. If a better aeroelastic model or a non-linear structural model is required then calculations must be performed at a range of frequencies. From this data a model of the solution in the frequency domain or time domain is obtained.

The construction of reduced order models (ROMs) using harmonic perturbation solutions has been achieved for a variety of flow equations via a number of techniques, most prominently via eigenmode summation and proper orthogonal decomposition [16]. Eigenmode summation has been used to reduce both the full potential [17] and Euler [18] equations. However, the application of proper orthogonal decomposition is increasingly investigated with models constructed for; a vortex lattice method [19], the full potential equations [17, 20], the Euler equations [21, 22] and the full potential equations coupled with an integral boundary layer model [23, 24]. Further improvements via balanced proper orthogonal decomposition [25] have also been obtained.

In the second approach, the one used in this work, the discrete time pulse responses (sample responses) of the unsteady linearized Euler system are calculated. Once the pulse responses of *any* linear system of equations are known the response of the same set of equations to any input can be predicted by convolution of the sample responses. The theory is described in detail by Silva [26], who applied the method to a full non-linear CFD scheme. Unlike the current work which calculates the sample response directly, Silva approximated the sample response of the linear system by using two sample responses of the non-linear system and assuming that the non-linearity was no more than second order. This work has been further developed by Raveh [27] and subsequently Silva [28] who showed that the sample response to an impulse in heave velocity for the AGARD 445.6 wing seemed sensitive to the choice of both time step size and the impulse amplitude used. The current method uses the linearized Euler equations and seems insensitive to the impulse amplitude, provided it is not so large as to cause unphysical surface pressures. It would be expected that both techniques would share the same time step dependence. However, no time step dependence has been found in this

or previous work [29, 30]. It is possible that the problems observed in References [27, 28] are a result of the fact the amplitude of the velocity pulse is a function of the time step and increases as the time step decreases. In the present work the velocity pulse amplitude is not a function of time step.

The computational efficiency of constructing a ROM using the convolution of sample responses is inversely proportional to the number of time steps calculated. It was found when reconstructing solutions for non-periodic motions that long sample response histories were required. The number of time steps required could be reduced by fitting an exponentially decaying component to the end of a truncated sample response but this seemed too *ad hoc*. Inspection of the sample responses suggested only a few modes were dominant, therefore standard system identification techniques could produce ROMs from smaller sample response histories than reconstruction via convolution.

Here, using a finite difference approximation to the time derivative the continuous equations are put into discrete form. The sample responses are in fact the discrete system Markov parameters and can be used to generate the Hankel matrices of the discrete system. The Eigensystem Realization Algorithm (ERA) [31], is used to realize the discrete time linearized unsteady aerodynamic system. ERA's are commonly used to realize or identify discrete-time state-space systems that describe the modal dynamics of a structure. The ERA requires a singular value decomposition of one of the Hankel matrices and a discrete ROM, of rank n, can then be obtained by retaining only the first n singular values. This results in a reduction in the number of unknowns from tens of thousands to tens. A similar approach has been used by Silva and Raveh [32]. This discrete system realization and any ROMs are valid for only one time step size. This fixed time step means that the discrete ROM cannot be accurately applied to structural models with discrete non-linearities (such as freeplay in a control surface). Any aerodynamic model must capture the 'switching' points between discrete regions [33] or unphysical limit cycle behaviour may be introduced into the solution [34]. Hence, since this is the type of problem for which the current method is being developed, the discrete model is merely used to derive a continuous ROM.

The mapping of the full continuous system matrices to the full discrete system matrices is one-to-one, so the inverse mapping is applied to the discrete ROM to give a valid continuous ROM. All the terms of the continuous system will be present if the ROM is large enough, but the size of time step and Hankel matrix used to derive the ROM will affect which terms are neglected. This, reduced, continuous model could then be put into a discrete form for varying time steps and/or different finite difference schemes.

2. CONTINUOUS LINEAR EULER EQUATIONS

The system reduction scheme described here could be applied to any suitable set of continuous linear differential equations. Here the linearized Euler equations (also sometimes called the small disturbance Euler equations) on moving meshes for an aerofoil which can undergo heave or linearized pitch motions are considered [29, 30]. It should be noted that these equations are spatially discrete, but continuous in time. For simplicity throughout this paper references to continuous or discrete models/systems indicate only the time dependent nature of the system.

First a steady reference state is calculated from the full non-linear integral Euler equations using a standard cell-centred finite-volume scheme [35]. Unsteady solutions are found by

regarding flow quantities as the sum of the steady or mean flow solution and an unsteady perturbation. The unsteady Euler equations are then linearized assuming that all unsteady perturbations, grid displacements and speeds are small. No assumption is made about the form of the perturbations. The non-linearity of the flow is contained in the steady solution and is therefore present in the unsteady solution. The boundary conditions are obtained by linearizing the actual boundary conditions used in the full unsteady code from which the linearized scheme is derived. The conditions used in the full code at walls are flow tangency, density set equal to that at the centre of the first cell adjacent to the wall and pressure is extrapolated using values in three cells adjacent to the wall. At the farfield boundary Riemann invariant boundary conditions are used. Details of the linearization process are given by Gaitonde and Jones [29].

The state-space representation of this system is given by

$$\begin{aligned} \dot{\mathbf{x}}(t) &= \mathbf{A}\mathbf{x}(t) + \mathbf{B}\mathbf{u}(t) \\ \mathbf{y}(t) &= \mathbf{C}\mathbf{x}(t) + \mathbf{D}\mathbf{u}(t) \end{aligned} \tag{1}$$

$\mathbf{A}, \mathbf{B}, \mathbf{C}$ and $\mathbf{D}$ are the system matrices. The input vector $\mathbf{u}$ and the state-vector $\mathbf{x}$ are given by

$$\mathbf{u} = \begin{bmatrix} h \\ \alpha \\ \dot{h} \\ \dot{\alpha} \end{bmatrix} \quad \mathbf{x} = \begin{bmatrix} \hat{\rho}_{2,2} \\ \hat{u}_{2,2} \\ \hat{v}_{2,2} \\ \hat{p}_{2,2} \\ \cdot \\ \cdot \\ \cdot \\ \hat{\rho}_{i\max,j\max} \\ \hat{u}_{i\max,j\max} \\ \hat{v}_{i\max,j\max} \\ \hat{p}_{i\max,j\max} \end{bmatrix} \tag{2}$$

where h is the heave displacement, α is the pitch angle, $\hat{\rho}$ $\hat{u}$, $\hat{v}$ and $\hat{p}$ are the changes from the mean values of the density, speeds and pressure. Note that the scheme considered here is a cell centred one, with centres inside the computational domain labelled $i = 2, i\max$, $j = 2, j\max$.

The vector $\mathbf{y}$ is the output and is defined to produce the required information about the linear system. An example of a suitable $\mathbf{y}$ is

$$\mathbf{y} = \begin{bmatrix} \hat{C}_\mathrm{l} \\ \hat{C}_\mathrm{d} \\ \hat{C}_\mathrm{m} \end{bmatrix} \tag{3}$$

where $\hat{C}_\mathrm{l}$, $\hat{C}_\mathrm{d}$ and $\hat{C}_\mathrm{m}$ are the changes in the lift, drag and moment coefficients from the mean values.

Then provided the entries of $\mathbf{Du}(t)$ are continuous for $t>0$, the output equation can be written as

$$\mathbf{y}(t)=\int_0^t \mathbf{H}(t-\tau)\mathbf{u}(\tau)\,\mathrm{d}\tau \tag{4}$$

Note the matrix $\mathbf{H}(t)$ has, as its ith column, the output response of the system for a unit impulse input $\delta(t)$ on the ith component of $\mathbf{u}$.

It can be shown [36] that

$$\begin{aligned}\mathbf{y}(t)&=\mathbf{Du}(t)+\int_0^t\left(\mathbf{CB}+\frac{t-\tau}{1!}\mathbf{CAB}+\frac{(t-\tau)^2}{2!}\mathbf{CA}^2\mathbf{B}+\cdots\right)\mathbf{u}(\tau)\,\mathrm{d}\tau\\ \mathbf{y}(t)&=\mathbf{H}_0\mathbf{u}(t)+\int_0^t\left(\mathbf{H}_1+\frac{t-\tau}{1!}\mathbf{H}_2+\frac{(t-\tau)^2}{2!}\mathbf{H}_3+\cdots\right)\mathbf{u}(\tau)\,\mathrm{d}\tau\end{aligned} \tag{5}$$

where the sequence of matrices $\mathbf{H}_k, k=0,\infty$

$$\{\mathbf{H}_0,\mathbf{H}_1,\mathbf{H}_2,\ldots,\mathbf{H}_k,\ldots\}=\{\mathbf{D},\mathbf{CB},\mathbf{CAB},\ldots,\mathbf{CA}^{k-1}\mathbf{B},\ldots\} \tag{6}$$

is called the weighting sequence, the impulse-response sequence or the Markov sequence of the system. Given the continuous-time impulse response matrix $\mathbf{H}(t)$, the $\mathbf{H}_k$ are defined by

$$\begin{aligned}\mathbf{H}_k&=\left.\frac{\mathrm{d}^{k-1}}{\mathrm{d}t^{k-1}}\mathbf{H}(t)\right|_{t=0^+}\qquad k\geqslant 1\\ \mathbf{H}_0&=\int_{0-}^{0+}\mathbf{H}(t)\,\mathrm{d}t\end{aligned} \tag{7}$$

If the Markov parameters of a continuous system are known, then it is possible to construct the generalized Hankel matrix $\mathbf{H}_{rs}(k)$

$$\mathbf{H}_{rs}(k)=\begin{bmatrix}\mathbf{CA}^k\mathbf{B} & \mathbf{CA}^{k+t_1}\mathbf{B} & \mathbf{CA}^{k+t_2}\mathbf{B} & \cdots & \mathbf{CA}^{k+t_{s-1}}\mathbf{B}\\ \mathbf{CA}^{k+j_1}\mathbf{B} & \mathbf{CA}^{k+t_1+j_1}\mathbf{B} & \mathbf{CA}^{k+t_2+j_1}\mathbf{B} & \cdots & \mathbf{CA}^{k+t_{s-1}+j_1}\mathbf{B}\\ \cdot & \cdot & \cdot & & \cdot\\ \cdot & \cdot & \cdot & & \cdot\\ \cdot & \cdot & \cdot & & \cdot\\ \mathbf{CA}^{k+j_{r-1}}\mathbf{B} & \mathbf{CA}^{k+t_1+j_{r-1}}\mathbf{B} & \mathbf{CA}^{k+t_2+j_{r-1}}\mathbf{B} & \cdots & \mathbf{CA}^{k+t_{s-1}+j_{r-1}}\mathbf{B}\end{bmatrix} \tag{8}$$

where $j_i(i=1,r-1)$ and $t_i(i=1,s-1)$ are arbitrary integers to allow for a random distribution of Markov parameters [31], so

$$\mathbf{H}_{rs}(k-1)=\begin{bmatrix}\mathbf{H}_k & \mathbf{H}_{k+t_1} & \mathbf{H}_{k+t_2} & \cdots & \mathbf{H}_{k+t_{s-1}}\\ \mathbf{H}_{k+j_1} & \mathbf{H}_{k+t_1+j_1} & \mathbf{H}_{k+t_2+j_1} & \cdots & \mathbf{H}_{k+t_{s-1}+j_1}\\ \cdot & \cdot & \cdot & & \cdot\\ \cdot & \cdot & \cdot & & \cdot\\ \cdot & \cdot & \cdot & & \cdot\\ \mathbf{H}_{k+j_{r-1}} & \mathbf{H}_{k+t_1+j_{r-1}} & \mathbf{H}_{k+t_2+j_{r-1}} & \cdots & \mathbf{H}_{k+t_{s-1}+j_{r-1}}\end{bmatrix} \tag{9}$$

From this matrix it is possible to realize and reduce the system matrices [31]. The information required to construct this matrix is not always directly available.

3. A DISCRETE APPROXIMATION TO THE CONTINUOUS LINEAR SYSTEM

The continuous linearized Euler equations (1) are generally solved by putting them into a discrete form using a finite difference approximation to the original differential equations of the system (1). A previously developed code [29] was used as the basis for the work described here. It is modified to use a simple first order implicit approximation to the time derivative so

$$\begin{aligned} \frac{\tilde{\mathbf{x}}_k - \tilde{\mathbf{x}}_{k-1}}{\Delta t} &= \mathbf{A}\tilde{\mathbf{x}}_k + \mathbf{B}\tilde{\mathbf{u}}_k \\ \tilde{\mathbf{y}}_k &= \mathbf{C}\tilde{\mathbf{x}}_k + \mathbf{D}\tilde{\mathbf{u}}_k \end{aligned} \tag{10}$$

where $\tilde{\mathbf{x}}, \tilde{\mathbf{u}}$ and $\tilde{\mathbf{y}}$ are discrete approximations to the state, input and output vectors, respectively.

On rearranging this becomes

$$\begin{aligned} \tilde{\mathbf{x}}_k &= \tilde{\mathbf{A}}\tilde{\mathbf{x}}_{k-1} + \tilde{\mathbf{B}}\tilde{\mathbf{u}}_k \\ \tilde{\mathbf{y}}_k &= \tilde{\mathbf{C}}\tilde{\mathbf{x}}_k + \tilde{\mathbf{D}}\tilde{\mathbf{u}}_k \end{aligned} \tag{11}$$

where the discrete system matrices are given by

$$\begin{aligned} \tilde{\mathbf{A}} &= (\mathbf{I} - \mathbf{A}\Delta t)^{-1} \\ \tilde{\mathbf{B}} &= (\mathbf{I} - \mathbf{A}\Delta t)^{-1}\mathbf{B}\Delta t \\ \tilde{\mathbf{C}} &= \mathbf{C} \\ \tilde{\mathbf{D}} &= \mathbf{D} \end{aligned} \tag{12}$$

This can be solved using one-sided z-transforms [37, 38] to give the output equation

$$\tilde{\mathbf{y}}(k) = \sum_{n=0}^{k} \tilde{\mathbf{H}}(k-n)\tilde{\mathbf{u}}_n \tag{13}$$

The matrix $\tilde{\mathbf{H}}(k)$ is composed of columns which are the outputs for a unit sample pulse input (see Figure 1) on each input channel separately, i.e. the ith column is the output vector at time k for a unit sample input in the ith component of $\tilde{\mathbf{u}}$ with all other entries of $\tilde{\mathbf{u}}$ set to zero, see Aplevich [36].

Then if $\tilde{\mathbf{x}}_{-1} = 0$ it follows from (11) that

$$\begin{aligned} \tilde{\mathbf{y}}_0 &= \tilde{\mathbf{C}}\tilde{\mathbf{B}}\tilde{\mathbf{u}}_0 + \tilde{\mathbf{D}}\tilde{\mathbf{u}}_0 \\ \tilde{\mathbf{y}}_1 &= \tilde{\mathbf{C}}\tilde{\mathbf{A}}\tilde{\mathbf{B}}\tilde{\mathbf{u}}_0 + \tilde{\mathbf{C}}\tilde{\mathbf{B}}\tilde{\mathbf{u}}_1 + \tilde{\mathbf{D}}\tilde{\mathbf{u}}_1 \\ \tilde{\mathbf{y}}_2 &= \tilde{\mathbf{C}}\tilde{\mathbf{A}}^2\tilde{\mathbf{B}}\tilde{\mathbf{u}}_0 + \tilde{\mathbf{C}}\tilde{\mathbf{A}}\tilde{\mathbf{B}}\tilde{\mathbf{u}}_1 + \tilde{\mathbf{C}}\tilde{\mathbf{B}}\tilde{\mathbf{u}}_2 + \tilde{\mathbf{D}}\tilde{\mathbf{u}}_2 \\ \tilde{\mathbf{y}}_3 &= \tilde{\mathbf{C}}\tilde{\mathbf{A}}^3\tilde{\mathbf{B}}\tilde{\mathbf{u}}_0 + \tilde{\mathbf{C}}\tilde{\mathbf{A}}^2\tilde{\mathbf{B}}\tilde{\mathbf{u}}_1 + \tilde{\mathbf{C}}\tilde{\mathbf{A}}\tilde{\mathbf{B}}\tilde{\mathbf{u}}_2 + \tilde{\mathbf{C}}\tilde{\mathbf{B}}\tilde{\mathbf{u}}_3 + \tilde{\mathbf{D}}\tilde{\mathbf{u}}_3 \end{aligned} \tag{14}$$

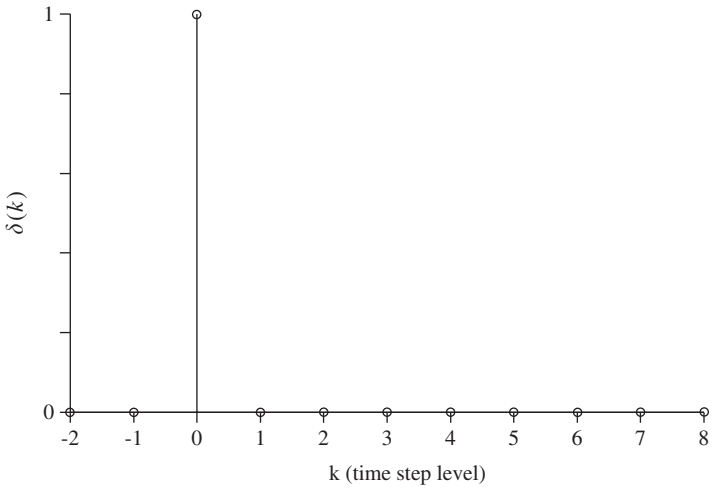

Figure 1. Unit sample pulse function $\sum_k \delta(k) = 1$.

Thus

$$\tilde{\mathbf{y}}_l = [\tilde{\mathbf{C}}\tilde{\mathbf{A}}^l\tilde{\mathbf{B}}, \tilde{\mathbf{C}}\tilde{\mathbf{A}}^{l-1}\tilde{\mathbf{B}}, \ldots, \tilde{\mathbf{C}}\tilde{\mathbf{A}}^2\tilde{\mathbf{B}}, \tilde{\mathbf{C}}\tilde{\mathbf{A}}\tilde{\mathbf{B}}, \tilde{\mathbf{C}}\tilde{\mathbf{B}} + \tilde{\mathbf{D}}] \begin{bmatrix} \tilde{\mathbf{u}}_0 \\ \tilde{\mathbf{u}}_1 \\ \cdot \\ \cdot \\ \cdot \\ \tilde{\mathbf{u}}_{l-2} \\ \tilde{\mathbf{u}}_{l-1} \\ \tilde{\mathbf{u}}_l \end{bmatrix} \tag{15}$$

The following sequence $\mathbf{H}_k, k = 0, \infty$

$$\{\mathbf{H}_0, \mathbf{H}_1, \mathbf{H}_2, \ldots, \mathbf{H}_k, \ldots\} = \{\tilde{\mathbf{D}} + \tilde{\mathbf{C}}\tilde{\mathbf{B}}, \tilde{\mathbf{C}}\tilde{\mathbf{A}}\tilde{\mathbf{B}}, \ldots, \tilde{\mathbf{C}}\tilde{\mathbf{A}}^k\tilde{\mathbf{B}}, \ldots\} \tag{16}$$

is the Markov sequence of the discrete system. The forced response of the discrete system is uniquely determined by its Markov sequence and the input. Thus any two systems with identical weighting sequences have identical forced responses for the same input. Note that for a system of rank n the sequence $\mathbf{H}_k, k = 0, 2n$ specifies the forced response exactly.

The system realization method described by Juang and Pappa relies on being able to construct the generalized Hankel matrix with the structure given in Equation (8) replacing continuous matrices with the discrete system matrices. For this implicit finite difference approximation it is possible to construct the required matrix by modifying the system since $\mathbf{D}$ and thus $\tilde{\mathbf{D}}$ are known matrices. For both the continuous system and the discrete approximation a modified output is defined by subtracting the term $\mathbf{Du}(t)$ from the continuous output and the term $\tilde{\mathbf{D}}\tilde{\mathbf{u}}$

from the discrete output equation. The modified discrete system is then

$$\begin{aligned}\tilde{\mathbf{x}}_k &= \tilde{\mathbf{A}}\tilde{\mathbf{x}}_{k-1} + \tilde{\mathbf{B}}\tilde{\mathbf{u}}_k \\ \tilde{\mathbf{y}}'_k &= \tilde{\mathbf{y}}_k - \tilde{\mathbf{D}}\tilde{\mathbf{u}}_k = \tilde{\mathbf{C}}\tilde{\mathbf{x}}_k\end{aligned} \tag{17}$$

Then

$$\tilde{\mathbf{y}}'_l = [\tilde{\mathbf{C}}\tilde{\mathbf{A}}^{l}\tilde{\mathbf{B}}, \tilde{\mathbf{C}}\tilde{\mathbf{A}}^{l-1}\tilde{\mathbf{B}}, \ldots, \tilde{\mathbf{C}}\tilde{\mathbf{A}}^{2}\tilde{\mathbf{B}}, \tilde{\mathbf{C}}\tilde{\mathbf{A}}\tilde{\mathbf{B}}, \tilde{\mathbf{C}}\tilde{\mathbf{B}}] \begin{bmatrix} \tilde{\mathbf{u}}_0 \\ \tilde{\mathbf{u}}_1 \\ \cdot \\ \cdot \\ \cdot \\ \tilde{\mathbf{u}}_{l-2} \\ \tilde{\mathbf{u}}_{l-1} \\ \tilde{\mathbf{u}}_l \end{bmatrix} \tag{18}$$

and the modified Markov sequence is

$$\{\mathbf{H}_0, \mathbf{H}_1, \mathbf{H}_2, \ldots, \mathbf{H}_k, \ldots\} = \{\tilde{\mathbf{C}}\tilde{\mathbf{B}}, \tilde{\mathbf{C}}\tilde{\mathbf{A}}\tilde{\mathbf{B}}, \ldots, \tilde{\mathbf{C}}\tilde{\mathbf{A}}^{k}\tilde{\mathbf{B}}, \ldots\} \tag{19}$$

The Hankel matrix in this case is the $r \times s$ block matrix given by

$$\mathbf{H}_{rs}(k) = \begin{bmatrix} \mathbf{H}_k & \mathbf{H}_{k+t_1} & \mathbf{H}_{k+t_2} & \cdots & \mathbf{H}_{k+t_{s-1}} \\ \mathbf{H}_{k+j_1} & \mathbf{H}_{k+t_1+j_1} & \mathbf{H}_{k+t_2+j_1} & \cdots & \mathbf{H}_{k+t_{s-1}+j_1} \\ \cdot & \cdot & \cdot & & \cdot \\ \cdot & \cdot & \cdot & & \cdot \\ \cdot & \cdot & \cdot & & \cdot \\ \mathbf{H}_{k+j_{r-1}} & \mathbf{H}_{k+t_1+j_{r-1}} & \mathbf{H}_{k+t_2+j_{r-1}} & \cdots & \mathbf{H}_{k+t_{s-1}+j_{r-1}} \end{bmatrix} \tag{20}$$

It is common to actually set $j_i = i$ and $t_i = i$ so that the Hankel matrix is

$$\mathbf{H}_{rs}(k) = \begin{bmatrix} \mathbf{H}_k & \mathbf{H}_{k+1} & \mathbf{H}_{k+2} & \cdots & \mathbf{H}_{k+s-1} \\ \mathbf{H}_{k+1} & \mathbf{H}_{k+2} & \mathbf{H}_{k+3} & \cdots & \mathbf{H}_{k+s} \\ \cdot & \cdot & \cdot & & \cdot \\ \cdot & \cdot & \cdot & & \cdot \\ \cdot & \cdot & \cdot & & \cdot \\ \mathbf{H}_{k+r-1} & \mathbf{H}_{k+r} & \mathbf{H}_{k+r+1} & \cdots & \mathbf{H}_{k+s+r-2} \end{bmatrix} \tag{21}$$

The continuous (9) and implicit (20) definitions of $\mathbf{H}_{rs}(k)$ differ in their relationship to the Markov parameters, however when the expressions for these parameters in terms of $\mathbf{A}, \mathbf{B}, \mathbf{C}$ or $\tilde{\mathbf{A}}, \tilde{\mathbf{B}}, \tilde{\mathbf{C}}$ are substituted then in both cases $\mathbf{H}_{rs}(k)$ has the same form. This matrix can be used to realise and reduce the system matrices [31].

4. SYSTEM REALIZATION AND REDUCTION

The Eigenvalue Realization Algorithm [31] provides a method for the system matrices (continuous or discrete) to be realized or identified provided the Hankel matrices can be constructed. This requires only knowledge of the Markov parameters of the system.

Focusing on the discrete system, the Markov parameters are matrices with columns equal to the value of the output vector $\tilde{\mathbf{y}}'$ for unit sample impulses on each component of $\tilde{\mathbf{u}}$ in turn. Note that the triple $[\tilde{\mathbf{A}}, \tilde{\mathbf{B}}, \tilde{\mathbf{C}}]$ is not unique and that for any non-singular matrix $\mathbf{T}$ the triple $[\mathbf{T}\tilde{\mathbf{A}}\mathbf{T}^{-1}, \mathbf{T}\tilde{\mathbf{B}}, \tilde{\mathbf{C}}\mathbf{T}^{-1}]$ is also a realization. Only a brief outline of the theory is given here. Given that the Hankel matrices are available the next step is to carry out a singular value decomposition (SVD) of $\mathbf{H}_{rs}(0)$. It is necessary to identify the size of this matrix. If there are p outputs and m inputs to the system then each of the Markov parameters is of size $p \times m$. Thus the size of the Hankel matrix is $rp \times sm$. Then the SVD is given by

$$\mathbf{H}_{rs}(0) = \mathbf{U}\mathbf{W}\mathbf{V}^{\mathrm{T}} \tag{22}$$

where $\mathbf{W}$ is an $sm \times sm$ diagonal matrix whose diagonal entries are called singular values which are either positive or zero, $\mathbf{U}$ is $rp \times sm$ and $\mathbf{V}$ is a $sm \times sm$ matrix. The SVD scheme is such that the elements of $\mathbf{W}$ are in size order i.e. $[w(1,1) > w(2,2) > w(3,3) \cdots]$. The rank of the reduced order model of the system is then determined by the number of elements of $\mathbf{W}$ which are larger than some desired accuracy or by taking into account only the n largest singular values in $\mathbf{W}$. Then partitioning the matrices

$$\begin{aligned}\mathbf{H}_{rs}(0) &= [\mathbf{P}\mathbf{P}'] \begin{bmatrix} \mathbf{\Lambda}_{n\times n} & \mathbf{O}_{n\times sm-n} \\ \mathbf{O}_{rp-n\times n} & \mathbf{\Lambda}'_{rp-n\times sm-n} \end{bmatrix} [\mathbf{Q}\mathbf{Q}']^{\mathrm{T}} \\ &= \mathbf{P}\mathbf{\Lambda}\mathbf{Q}^{\mathrm{T}} + \mathbf{P}'\mathbf{\Lambda}'\mathbf{Q}'^{\mathrm{T}} \end{aligned} \tag{23}$$

Now if matrix $\mathbf{H}_{rs}(0)$ can be approximated as

$$\mathbf{H}_{rs}(0) = \mathbf{P}\mathbf{\Lambda}\mathbf{Q}^{\mathrm{T}} \tag{24}$$

then matrices $\mathbf{U}, \mathbf{W}, \mathbf{V}$ can be reduced in size by deleting unnecessary columns and rows as appropriate. The reduced matrix from $\mathbf{U}$ is $\mathbf{P} : rp \times n$, the reduced matrix from $\mathbf{W}$ is $\mathbf{\Lambda} : n \times n$ and the reduced matrix from $\mathbf{V}$ is $\mathbf{Q} : sm \times n$.

It is then possible to show [31] that a realization is

$$\begin{aligned} \tilde{\mathbf{A}} &= \mathbf{\Lambda}^{-1/2}\mathbf{P}^{\mathrm{T}} H_{rs}(1)\mathbf{Q}\mathbf{\Lambda}^{-1/2} \\ \tilde{\mathbf{B}} &= \mathbf{\Lambda}^{1/2}\mathbf{Q}^{\mathrm{T}}\mathbf{E}_m \\ \tilde{\mathbf{C}} &= \mathbf{E}_p^{\mathrm{T}}\mathbf{P}\mathbf{\Lambda}^{1/2} \end{aligned} \tag{25}$$

where $\mathbf{E}_p = [\mathbf{I}_p, \mathbf{0}_p, \mathbf{0}_p, \ldots, \mathbf{0}_p]$ has size $p \times rp$ and $\mathbf{E}_m^{\mathrm{T}} = [\mathbf{I}_m, \mathbf{0}_m, \mathbf{0}_m, \ldots, \mathbf{0}_m]$ has size $m \times sm$. Thus it is possible to obtain a discrete ROM from the unit sample responses of the discrete CFD scheme. This model could be used for a range of test cases. It would however fix the discretization scheme used and the time step for the output.

A ROM of the continuous system is obtained by applying the inverse of the relationship between the continuous and discrete system matrices (12) to the discrete ROM matrices.

This is a valid realization of the continuous system. However the terms which have been omitted from the reduced size discrete system Hankel matrix may not be exactly the same terms which would have been omitted from the equivalent continuous Hankel matrix. In other words there may be some differences between a rank n system ($n < rank(\mathbf{A})$) obtained from the discrete system Hankel matrix and a rank n system obtained directly from the continuous system Hankel matrix. However it is probable that the dominant terms will be correctly predicted. Since all the terms of the continuous system would be present for a sufficiently large realization, by taking an appropriately sized ROM a continuous ROM of acceptable accuracy can be obtained. This continuous system ROM could be used with different time steps and even different finite difference schemes.

5. SYSTEM INPUT CHANNELS

In this section the required independent input channels for motions which are a combination of arbitrary heave and linearized pitch motions are identified and the required inputs to the program given. Note that whilst in the above a unit impulse applied at time zero was considered, the input can actually be applied at any time $k\Delta t$ and be of any size (with the corresponding response in the convolution sum scaled accordingly). In some cases an impulse of unit size might be too large as the pressures may become negative during the initial pseudo-time iterations leading to divergence of the numerical scheme. Thus a much smaller size of impulse is applied. Note that since the linearized code made no assumption about the form of the grid perturbations or speeds a wider range of problems may be tackled directly than is possible with a linearized harmonic code.

For the motions considered here, the displacement at any time is

$$\begin{aligned} \Delta x &= (\bar{y} - b_c)\alpha_{\text{amp}}(t) \\ \Delta y &= -(\bar{x} - a_c)\alpha_{\text{amp}}(t) + h(t) \end{aligned} \tag{26}$$

and the speeds are

$$\begin{aligned} \dot{x} &= (\bar{y} - b_c)\dot{\alpha}_{\text{amp}}(t) \\ \dot{y} &= -(\bar{x} - a_c)\dot{\alpha}_{\text{amp}}(t) + \dot{h}(t) \end{aligned} \tag{27}$$

There are four associated input channels for this flow, the pulse inputs are given in Table I where c_1, c_2, c_3 and c_4 are scaling constants. These scaling constants were necessary because putting a unit size pulse on each input could lead to divergence of the numerical scheme. The scheme at each real time step imposes the wall boundary conditions in full at the start of the pseudo time iterations. If the imposed displacement or speed was too large this could lead to unphysical negative pressures at the start of the calculations which could lead to failure of the solution process. It was found that unit angle motion in degrees was acceptable, but unit heave or speeds was too large. Due to the fact that the scheme is linear the solution for any input is just a scaled to produce the solution at any other input. Thus smaller values were thus used for some quantities to ensure easy convergence of the numerical scheme.

Table I. Channel inputs to the linearized Euler equations for heave and linearized pitch motions.

	Channel 1 h	Channel 2 $\dot{h}$	Channel 3 α	Channel 4 $\dot{\alpha}$	All Channels $h, \dot{h}, \alpha, \dot{\alpha}$
	$t = k\Delta t$	$t = k\Delta t$	$t = k\Delta t$	$t = k\Delta t$	$t \neq k\Delta t$
Δx	0	0	$(\bar{y} - b_c)c_3$	0	0
Δy	c_1	0	$-(\bar{x} - a_c)c_3$	0	0
x_t	0	0	0	$(\bar{y} - b_c)c_4$	0
y_t	0	c_2	0	$-(\bar{x} - a_c)c_4$	0

6. RESULTS

The test cases shown here are for a NACA64A010 aerofoil with freestream Mach number $M_\infty = 0.796$. The grid used for the majority of calculations is of size 191×36, this means that the number of unknowns is 26 600. A steady calculation is performed for the aerofoil at incidence $\alpha = 0°$. The steady flow is symmetric and has a shockwave near the midchord, see Figures 2 and 3.

The sample responses for each of the four input channels are calculated (two for heave and two for linear pitch) see Figure 4. The non-dimensional time step used to calculate these responses is $\Delta t_1 = (\Delta t_1^{\dim}/c)\sqrt{p_\infty/\rho_\infty} = 0.23$ where the superscript dim represents the dimensional quantity and c is the chord. Note that the scaling constants used are $c_1 = 0.1$, $c_2 = 0.1$, $c_3 = \pi/180$ and $c_4 = 0.38\pi/180$. These sample responses were then used to generate continuous ROMs of the flow.

6.1. Pulse responses with different time steps

As an initial test the continuous ROMs, created using a pulse width of Δt_1, were used to calculate sample responses for pulses of different effective widths, Δt. In other words by using a different time step and applying a unit sample function on each input channel the finite difference scheme sees a pulse of different duration or width. For the first case shown in Figure 5 the time step used is $\Delta t = \Delta t_1/5$ and for the second case shown in Figure 6 the time step used is $\Delta t = 5\Delta t_1$. Results from a full linearized Euler calculation and two ROMs of different sizes calculated from Hankel matrices using the first 40 terms of the sample responses are shown. In both figures there is good agreement between the α sample responses calculated from the rank 22 ROM and the linearized Euler solution. This illustrates the fact that the continuous ROM obtained from the discrete ROM with a particular time step can be discretized for both larger and smaller time steps and solved to give good solutions. The responses for input on the other input channels yield similar results.

6.2. Heave motions

The first heave motion is defined in dimensional variables by

$$h(t) = h_{\max} \sin(\omega t) \tag{28}$$

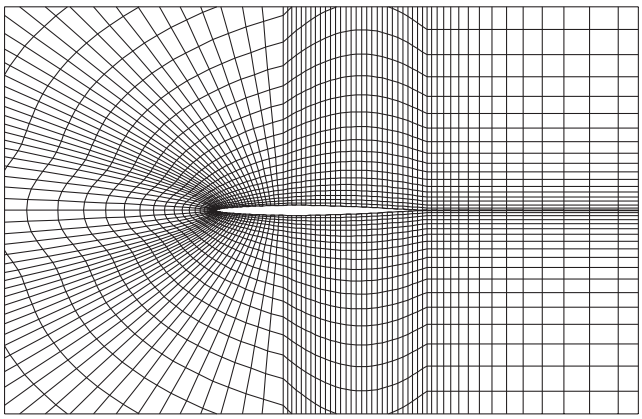

Figure 2. Mean grid.

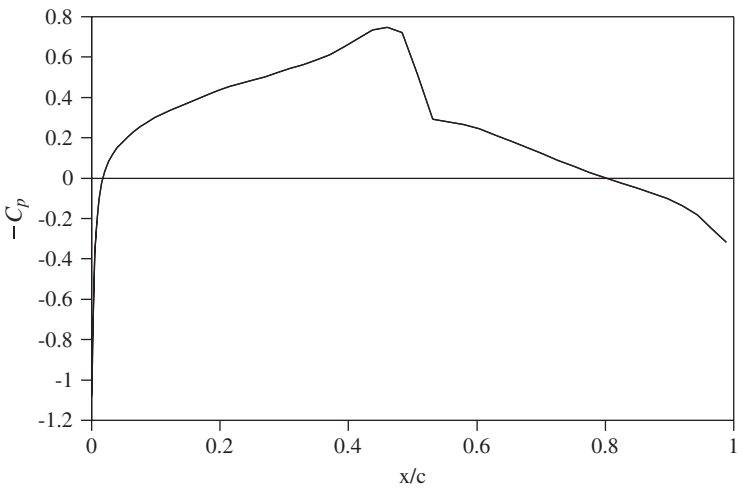

Figure 3. Mean solution, pressure coefficient distribution.

the amplitude of the motion is $h_{\max}/c = 0.05$, and the reduced frequency is $k_{\text{red}} = 0.202$. The reduced frequency is defined [39] as

$$k_{\text{red}} = \frac{\omega c}{2U_\infty} \tag{29}$$

The second motion considered is for a ramp in heave given in dimensional variables by

$$\begin{aligned} h(t) &= 0 && t < 0 \\ h(t) &= h_{\max}(1 - t_{\text{rat}}^2[2 - t_{\text{rat}}^2]) && 0 \leqslant t \leqslant 2t_{\text{ramp}} \\ h(t) &= 0 && t > 2t_{\text{ramp}} \end{aligned} \tag{30}$$

where $t_{\text{rat}} = (t - t_{\text{ramp}})/t_{\text{ramp}}$ and t_{ramp} is the ramp time. For the current case $h_{\max}/c = 0.01$ and the non-dimensional ramp time $t_{\text{ramp}}^{nd} = 5$.

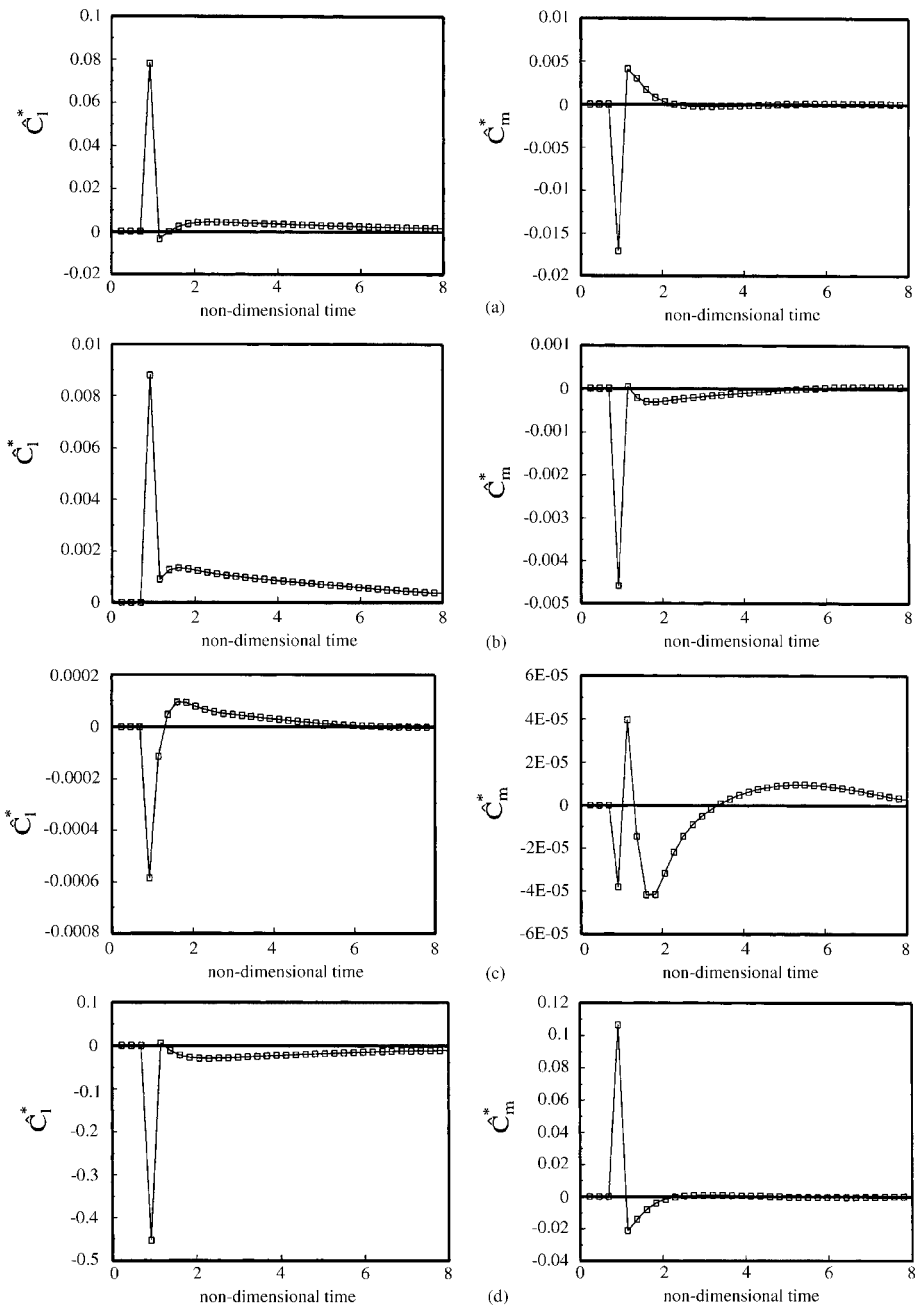

Figure 4. Sample responses calculated with time step $\Delta t_1 = 0.23$ (a) α pulse, (b) $\dot{\alpha}$ pulse, (c) h pulse and (d) $\dot{h}$ pulse.

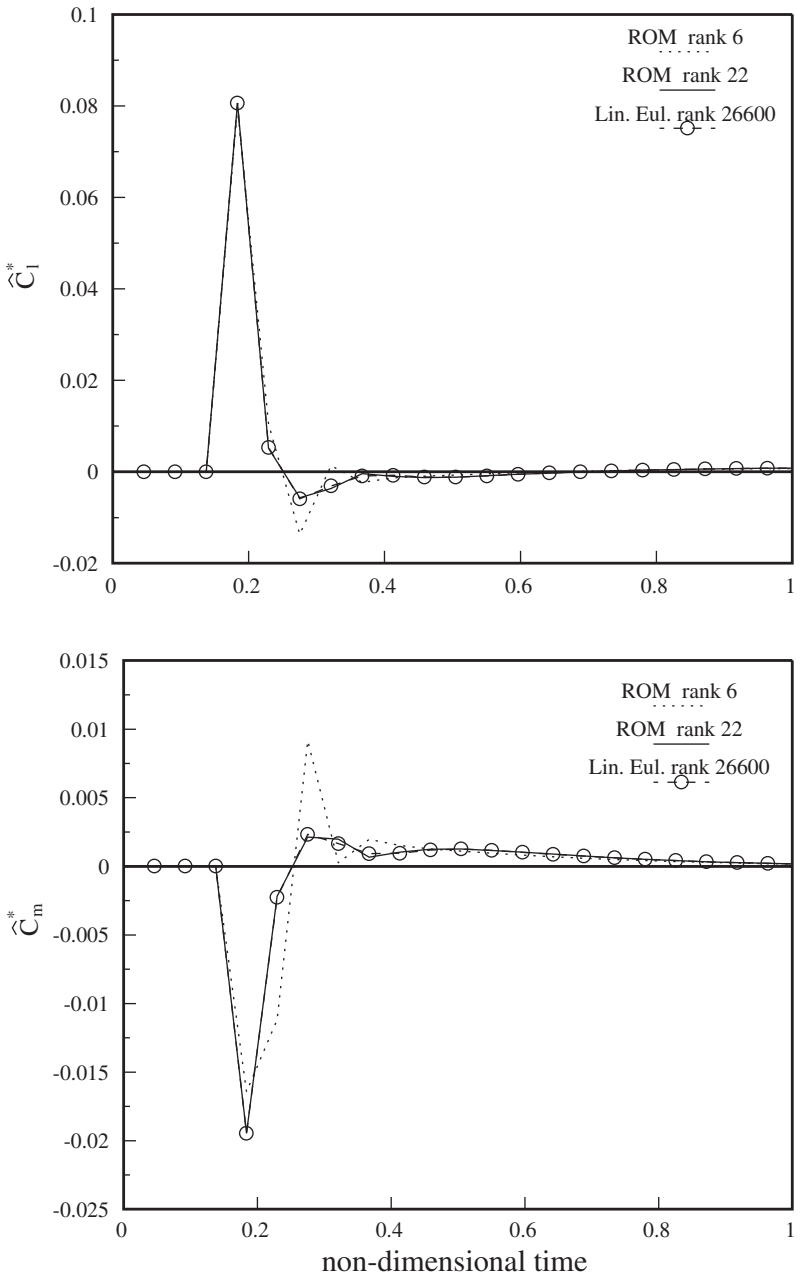

Figure 5. Comparison of α sample responses calculated directly from the linear Euler scheme and from ROMs for $\Delta t = \Delta t_1/5$.

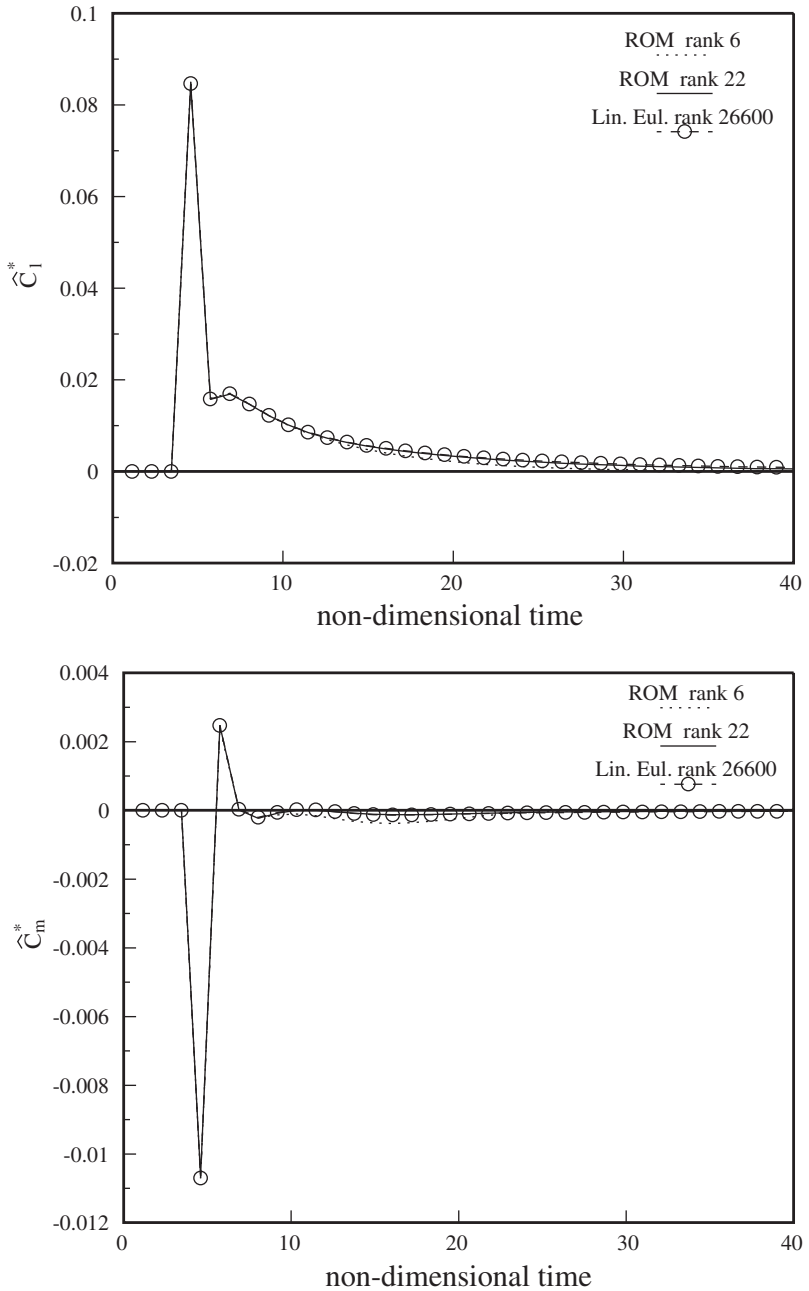

Figure 6. Comparison of α sample responses calculated directly from the linear Euler scheme and from ROMs for $\Delta t = 5\Delta t_1$.

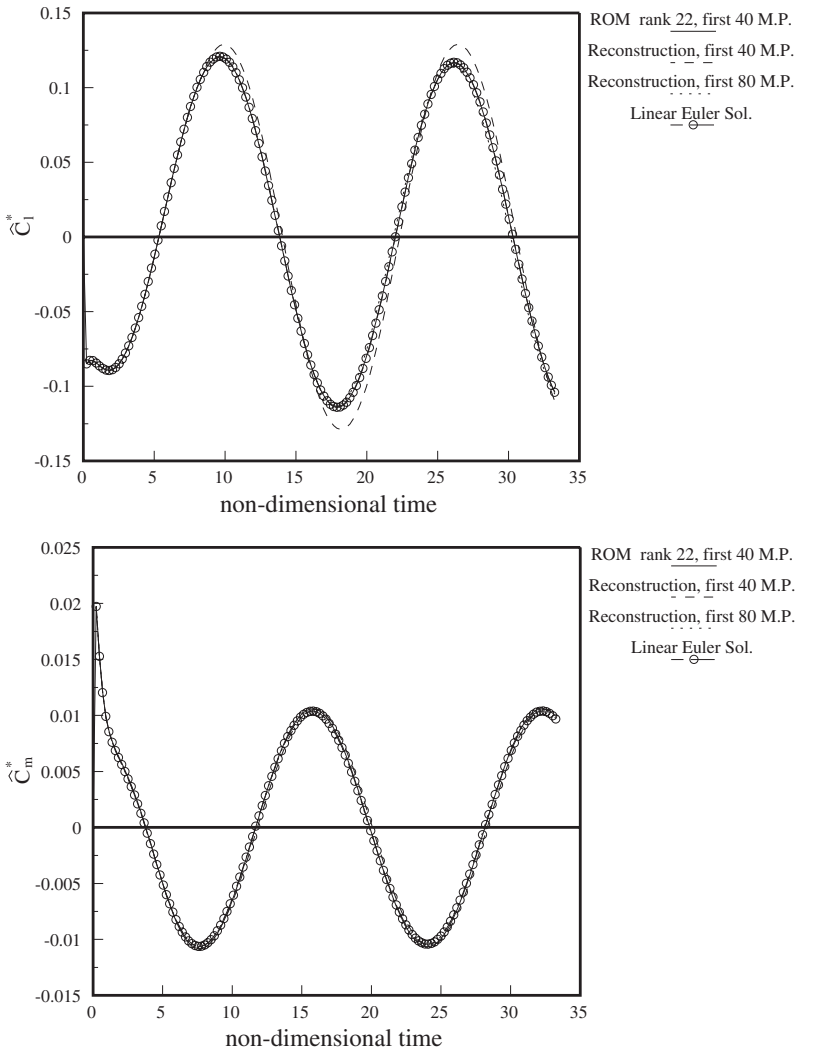

Figure 7. Comparison of solutions for an oscillatory heave motion calculated directly from the linear Euler scheme, from ROMs and from reconstructed summations.

For these cases comparisons between the linearized Euler solution, a ROM solution and solutions reconstructed by convolution of the unit sample responses with the general input are shown in Figures 7 and 8, respectively. The ROM used has rank 22 and was constructed using the first 40 Markov parameters (i.e. the first 40 terms of the sample responses). Two reconstructed solutions are calculated from truncated convolution summations using the first 40 and 80 Markov parameters. In both cases the ROM solution is in excellent agreement with the linear Euler solution. For the first test case the convolved solution using the same number of Markov parameters does show some differences, however using more terms leads to improved agreement. In the second test case both the convolved solutions deviate from the

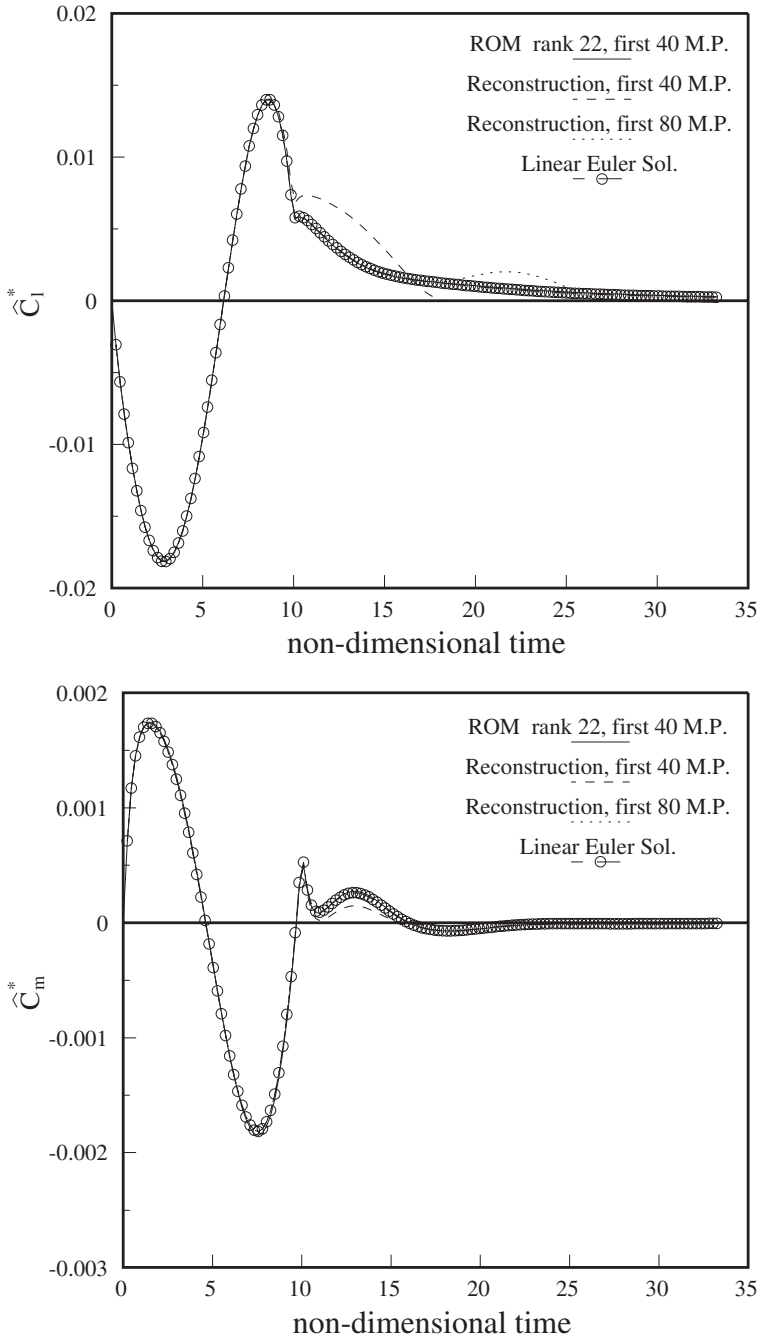

Figure 8. Comparison of solutions for a ramp heave motion calculated directly from the linear Euler scheme, from ROMs and from reconstructed summations.

linear Euler solution. The main reason for this is that the input to the system beyond the ramp is zero and so the only contribution to the convolution sum is from the ramp region which has non-zero input. Thus since these terms are multiplied by the Markov parameters which are furthest in time, when the number of Markov parameters used is truncated these non-zero terms are no longer included and inaccuracy results. A small number of Markov parameters can be forced to yield convolved solutions with improved accuracy provided an exponentially decaying component is fitted to the end of the truncated sample response.

6.3. *Heave and linear pitch motion*

The final case considered is a flow which is a combination of heave and linear pitch motions. The heave motion is an up and down ramp defined by Equation (30) with $t_{\text{ramp}} = 5$ and $h_{\max}/c = 0.1$. The pitch angle α undergoes a sinusoidal oscillation

$$\alpha(t) = \alpha_m + \alpha_0 \sin(\omega t) \tag{31}$$

where $\alpha_m = 0°$, $\alpha_0 = 0.5°$ and $k_{\text{red}} = 0.202$. The axis of rotation is located at $x/c = 0.25$.

This test case was calculated using both the usual 191×36 mesh and a finer 241×48 mesh. Using the first 40 Markov parameters continuous ROMs of various ranks are generated. The solutions are shown in Figures 9 and 10 for the coarse and fine meshes, respectively. In both cases, the lift perturbation coefficient is well predicted with a system of rank as low as 6, however the moment perturbation coefficient is not accurately predicted by the rank 6 system. Good agreement is achieved by the rank 14 and rank 22 systems. It can be seen that the trends are the same on both meshes. These results are consistent with Epureanu *et al.* [20] who observed that less accurate POD modes (from a small number of snapshots of the flow in the frequency domain) can be used provided that an increased number of degrees of freedom are used.

The instantaneous pressure distributions predicted by the full dynamically linear code at four times are shown in Figure 11. Pressure distributions are not available from the ROM since the only outputs are force coefficient values. These are the outputs which provide the required information for coupling with a simple structural model [7]. If a more sophisticated structural model was required then for example aerofoil surface pressures could be the ROM outputs. These pressure distributions illustrate the effects of the motion on the shock.

The rank of the system is then fixed at 14 and ROMs are generated using Hankel matrices of various sizes (or different numbers of Markov Parameters). The solutions are shown in Figures 12 and 13 with the block size of the Hankel matrix indicated (the number of Markov parameters required equals the sum of the number of block rows and columns). Note that each block is of size 3×4. For the 191×36 mesh, it can be seen that when using a 10×10 block Hankel matrix (the smallest possible for the current problem to generate a rank 14 ROM) the solution is unstable. For the other ROMs generated using larger Hankel matrices the solutions are stable and are in close agreement with the linear Euler solution. For the 241×48 mesh the solutions are all stable but the rank 6 solution is in poor agreement with the linear Euler solution. For the coarse mesh the Hankel singular values are shown in Figure 14 for the three Hankel matrices shown in Figure 12 together with those for a larger Hankel matrix of block size 25×25. It can be seen that as the size of the Hankel matrix increases, so there is a convergence of the calculated singular values. The instability of the ROM produced from the smallest Hankel matrix is possibly due to the fact that some of the singular values retained

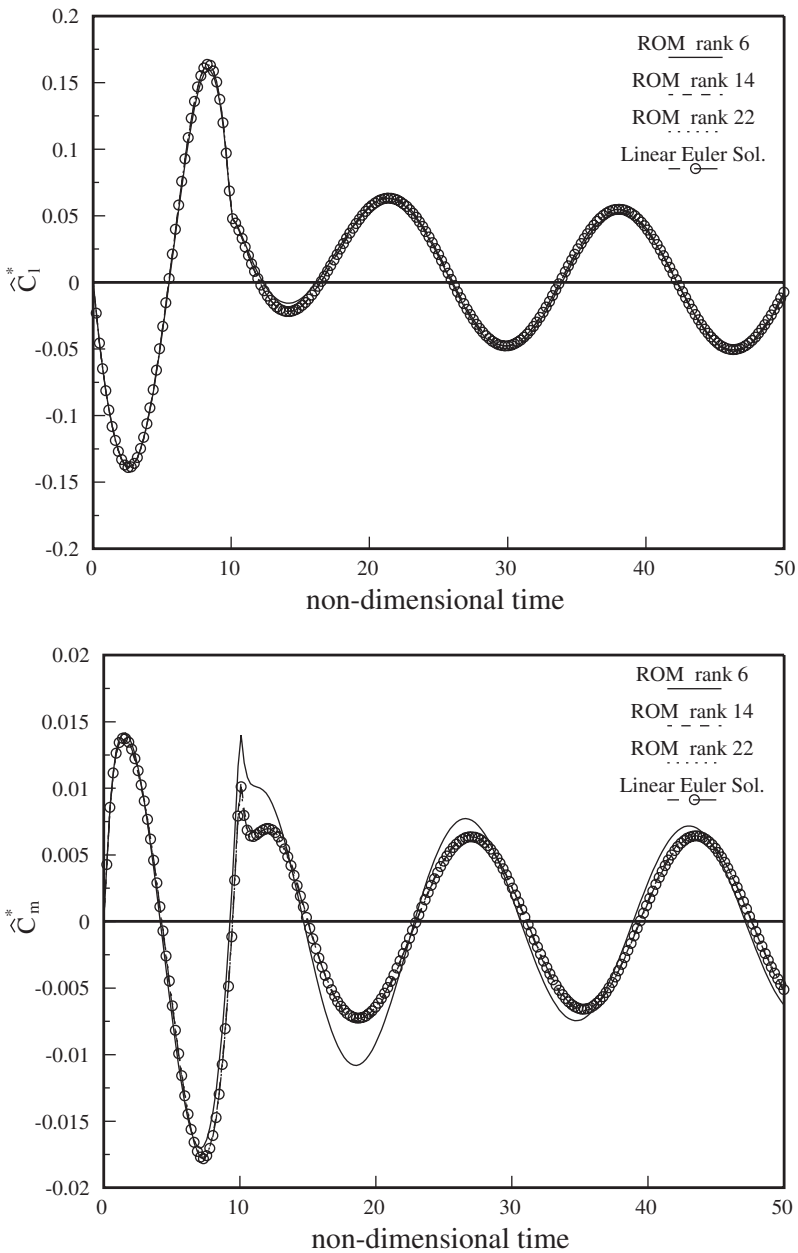

Figure 9. Comparison of solutions ROMs of various ranks calculated from the same Hankel matrix. Coarse mesh 191×36.

are not predicted accurately enough. This observation is similar to that of Epureanu *et al.* [20] who found that for POD that increasing the number of snapshots in the frequency domain improved the accuracy of POD modes.

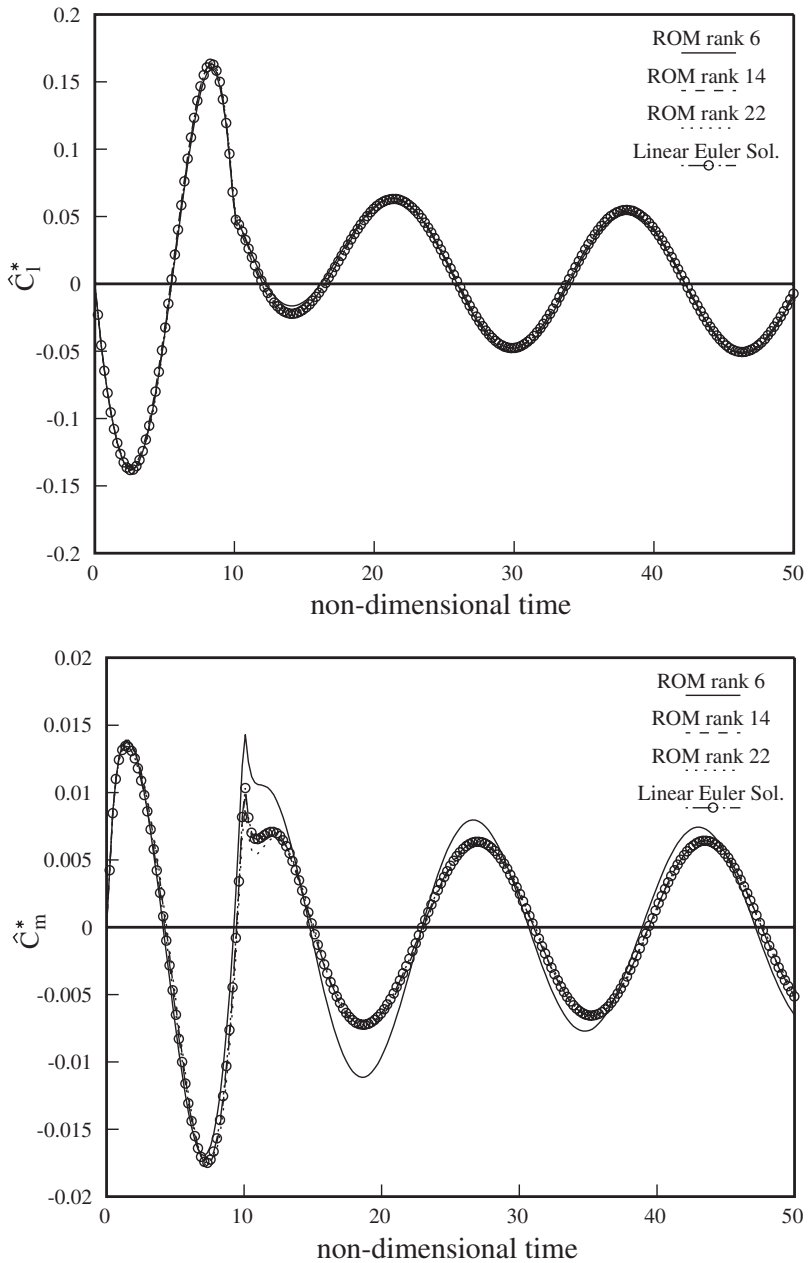

Figure 10. Comparison of solutions ROMs of various ranks calculated from the same Hankel matrix. Fine mesh 241×48.

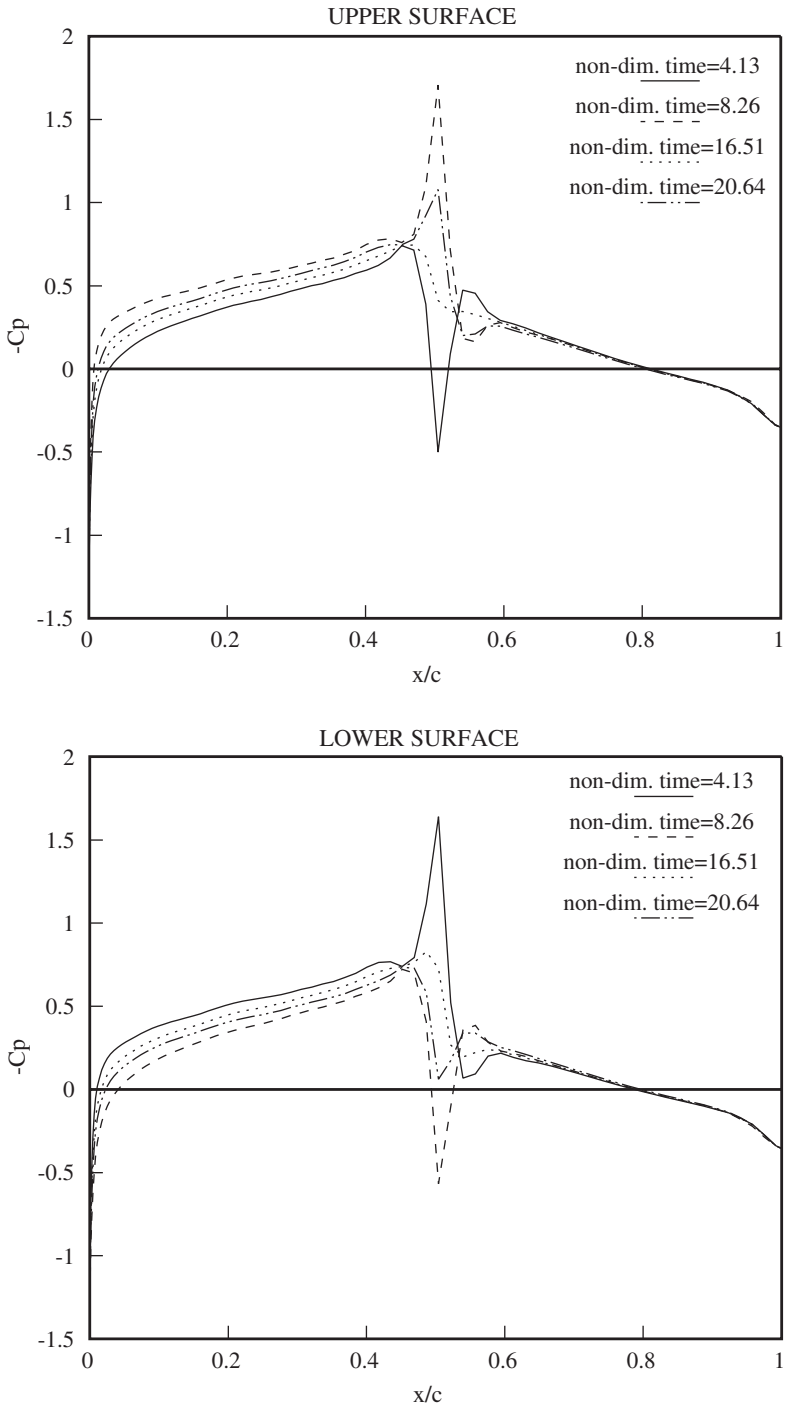

Figure 11. Upper and lower surface pressure distributions from full linear solution matrices. Fine mesh 241×48.

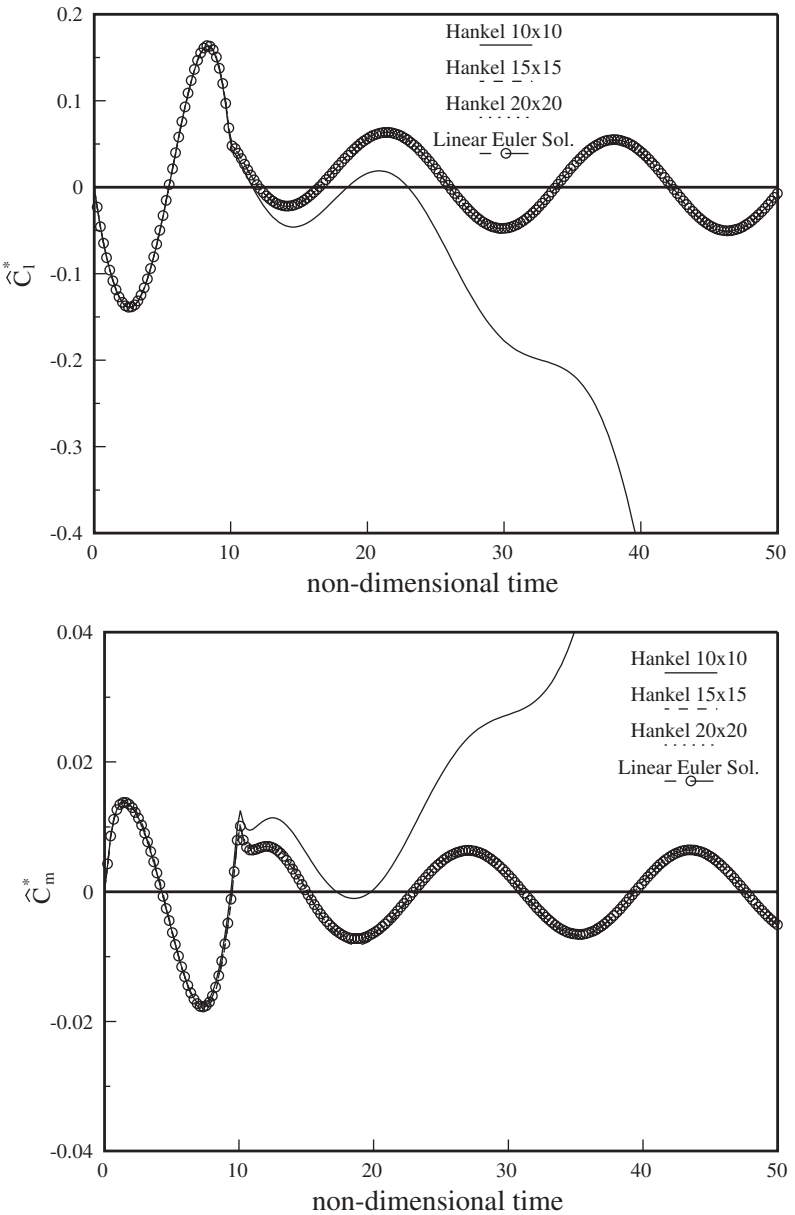

Figure 12. Comparison of solutions for rank 14 ROMs calculated from different Hankel matrices. Coarse mesh 191×36.

7. CONCLUSIONS

The method described in this paper for obtaining continuous ROMs of a linear CFD scheme has been shown to work and offers the possibility of efficient and flexible predictions of

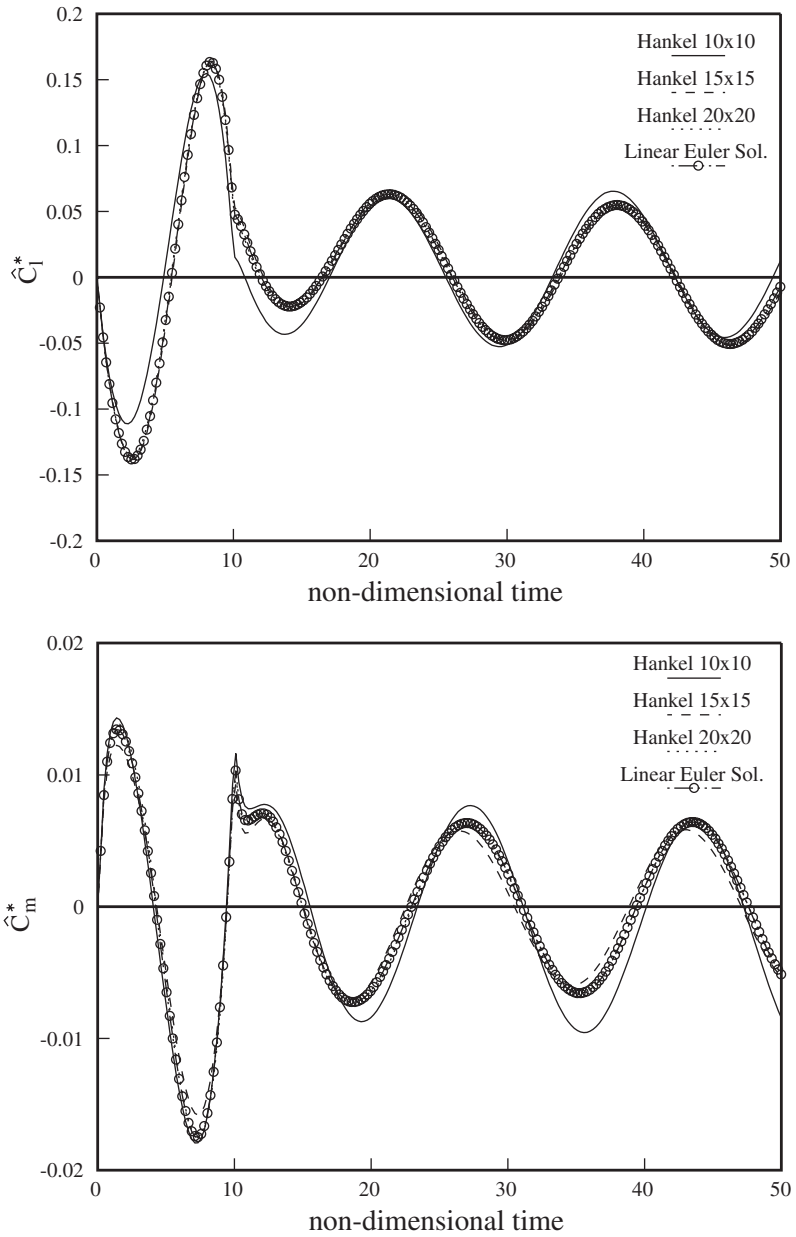

Figure 13. Comparison of solutions for rank 14 ROMs calculated from different Hankel matrices. Fine mesh 241×48.

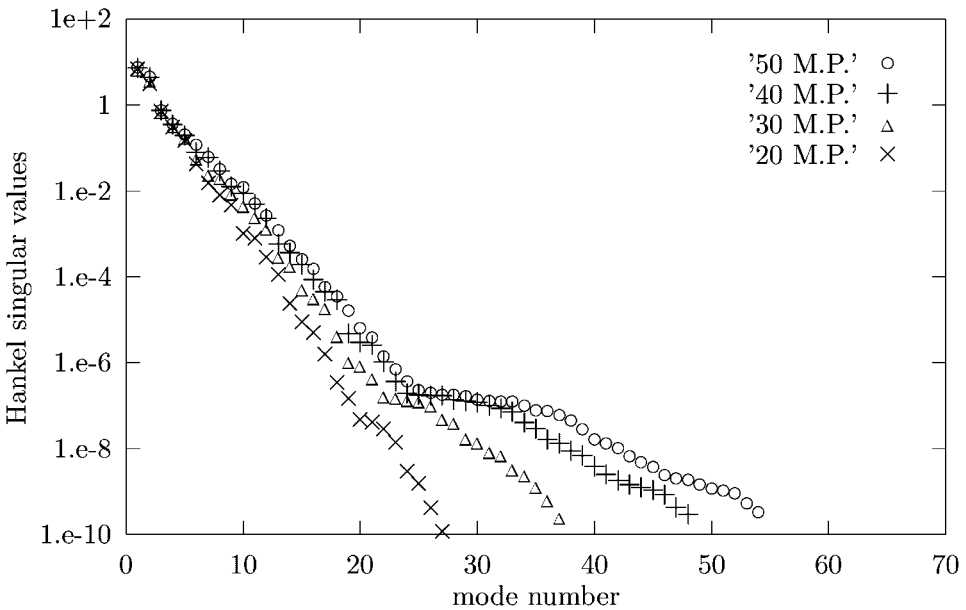

Figure 14. Singular values of Hankel matrix constructed using 20, 30, 40, 50 Markov parameters.

unsteady flows. The number of system unknowns is significantly reduced (from tens of thousands to tens for the test cases shown) and unlike discrete ROMs it can potentially be used with different time steps and finite different schemes. Since the number of unknowns required appears to be very small it represents a viable tool for structural coupling. Good agreement has recently been found between full-non-linear solutions and ROMs coupled with a structural model [7, 41]. The ROMs can be used to calculate LCOs due to structural non-linearities, but not those due to aerodynamic non-linearities. The work outlined here is part of an ongoing program. Further work is necessary to consider the effect of the time step size used in the calculation of pulse responses on the continuous ROM and the range of frequencies for which it is valid. Work is also currently being undertaken to look at obtaining continuous ROMs by either directly constructing the continuous Hankel matrix from the system matrices or by using a discrete explicit scheme [41]. Another area for future investigation is suggested by the work of Tang *et al.* [40] for a vortex lattice flow model. They obtain a continuous ROM from a discrete ROM by assuming that the discrete system is linked with a continuous system by the mapping commonly used in signal processing. This assumes that the output of the discrete scheme matches exactly the output of the continuous system at discrete time steps for a step-wise matched input. This would not truely be the case unless the continuous equations had been discretized in the required manner, which is not stated by Tang *et al.* However it appears to yield a reasonable system and thus is worthy of further investigation for the current scheme.

ACKNOWLEDGEMENTS

The authors wish to thank Walter Silva for useful discussions on the pulse responses.

REFERENCES

1. Venkatakrishnan V, Jameson A. Computation of unsteady transonic flows by the solution of the Euler equations. *AIAA Journal* 1998; **26**:974–981.
2. Brenneis A, Erbele A. Evaluation of an unsteady implicit Euler code against two and three-dimensional standard configurations. *AGARD CP-507* 1991; Paper 10.
3. Guruswamy GP. Unsteady aerodynamic and aeroelastic calculations for wings using Euler equations. *AIAA Journal* 1990; **28**:461–469.
4. Jameson AJ. Time dependent calculations using multigrid, with applications to unsteady flows past airfoils and wings. *AIAA Paper 91-1596*, 1991.
5. Gaitonde AL. A dual time method for the solution of the unsteady Euler equations. *Aeronautical Journal* 1994; **98**(978).
6. Dowell EH, Hall KC. Modelling of fluid-structure interation. *Annual Reviews in Fluid Mechanics* 2001; **33**:445–490.
7. Roberts I, Gaitonde AL, Jones DP, Lieven NAJ. *Identification of limit-cycles for piecewise nonlinear aeroelastic systems in transonic regimes*. CEAS Aerospace Aerodynamics Research Conference, Cambridge, 2002.
8. Kreiselmaier E, Laschka B. Small disturbance Euler equations: efficient and accurate tool for unsteady load prediction. *Journal of Aircraft* 2000; **37**(5):770–778.
9. Hall KC, Crawley EF. Calculation of unsteady flows in turbomachinery using the linearized Euler equations. *AIAA Journal* 1989; **27**(6).
10. Hall KC. A linearized Euler analysis of unsteady flows in turbomachinery. *Sc.D. Thesis*, Massachusetts Institute of Technology, USA, 1987.
11. Lindquist DR. Computation of unsteady transonic flowfields using shock capturing and the linear perturbation Euler equations. *Ph.D. Dissertation*, Department of Aeronautics and Astronautics, Massachusetts Institute of Technology, USA, 1991.
12. Lindquist DR, Giles MB. Validity of linearized unsteady Euler equations with shock capturing. *AIAA Journal* 1994; **32**(1).
13. Kahl G, Klose A. Time linearized Euler calculations for unsteady quasi-3D cascade flows. In *Sixth International Symposium on Unsteady Aerodynamics, Aeroacoustics and Aeroelasticity of Turbomachines and Propellors* (*Univ. of Notre Dame*, *1991*). Springer: Berlin, 1993.
14. Holmes DG, Chuang HA. Two-dimensional linearized harmonic Euler flow analysis for flutter and forced response. In *Sixth International Symposium on Unsteady Aerodynamics, Aeroacoustics and Aeroelasticity of Turbomachines and Propellors* (*Univ. of Notre Dame*, *1991*). Springer: Berlin, 1993.
15. Clark WS. Investigation of unsteady viscous flows in turbomachinery using a linearized Navier–Stokes analysis. *Ph.D. Thesis*, Duke University, USA, 1998.
16. Romanowski MC. Reduced order unsteady aerodynamic and aeroelastic models using Karhunen-Loeve eigenmodes. In *Proceedings of the Sixth AIAA Symposium on Multidisciplinary Analysis and Optimization*. AIAA paper 96-3981, 1996.
17. Hall KC, Florea R, Lanzkron PJ. A reduced order model of unsteady flows in turbomachinery. *Journal of Turbomachines* 1995; **117**(3):375–383.
18. Romanowski MC, Dowell EH. Reduced order Euler equations for unsteady aerodynamic flows: numerical techniques. *AIAA paper 96-0528*, 1996.
19. Kim T. Frequency-domain Karhunen-Loeve method and its application to linear dynamic systems. *AIAA Journal* 1998; **36**(11):2117–2123.
20. Epureanu BI, Dowell EH, Hall KC. A parametric analysis of reduced order models of potential flows in turbomachinery using proper orthogonal decomposition. ASME paper 2001-GT-0434, *Proceedings of ASME Turbo-expo 2001*, June 4–7, 2001, New Orleans, USA.
21. Hall KC, Thomas JP, Dowell EH. Reduced-order modeling of unsteady small disturbance flows using a frequency domain proper orthogonal decomposition technique. *AIAA Paper 99-0655*, 1999.
22. Hall KC, Thomas JP, Dowell EH. Proper orthogonal decomposition technique for transonic unsteady aerodynamic flows. *AIAA Journal* 2000; **38**(10):1853–1862.
23. Epureanu BI, Hall KC, Dowell EH. Reduced order models of unsteady transonic viscous flows in turbomachinery. *Journal of Fluids and Structures* 2000; **14**(8):1215–1235.
24. Epureanu BI, Hall KC, Dowell EH. Reduced order in turbomachinery using inviscid-viscous coupling. *Journal of Fluids and Structures* 2001; **15**(2):255–273.
25. Willcox K, Peraire J. Balanced model reduction via proper orthogonal decomposition. *AIAA Paper 2001-2611*, 2001.
26. Silva WA. Discrete-time linear and nonlinear aerodynamic impulse responses for efficient CFD analyses. *Ph.D. Thesis*, Department of Applied Science, College of William and Mary, Virginia, USA, 1997.
27. Raveh DE. Reduced-order models for nonlinear unsteady aerodynamics. *AIAA Journal* 2001; **39**(8).
28. Silva WA, Bartels RE. Development of reduced-order models for aeroelastic analysis and flutter prediction using the CFL3Dv6.0 code. *AIAA Paper 2002-1596*, 2002.

29. Gaitonde AL, Jones DP. Solutions of the 2D linearized unsteady Euler equations on moving meshes. *Proceedings of the Institution of Mechanical Engineering*, vol. 216, Part G. *Journal of Aerospace Engineering*, 2002.
30. Gaitonde AL, Jones DP. The use of pulse responses for 2D unsteady flows and system reduction. *The Aeronautical Journal*, Oct. 2002, to be published.
31. Juang J-N, Pappa RS. An eigensystem realization algorithm for modal parameter identification and model reduction. *Journal of Guidance*, *Control and Dynamics* 1985; **8**(5):620–627.
32. Silva WA, Raveh DE. Development of unsteady aerodynamic state-space models from CFD-based pulse responses, *AIAA Paper 2001-1213*, 2001.
33. Conner MD, Virgin LN, Dowell EH. Accurate numerical integration of state-space models for aeroelastic systems with freeplay. *AIAA Journal* 1996; **34**(10):2202–2205.
34. Lin WB, Cheng WH. Nonlinear flutter of loaded lifting surfaces (I) & (II). *Journal of the Chinese Society of Mechanical Engineering* 1993; **14**(5):446–466.
35. Jameson A, Schmidt W, Turkel E. Numerical solutions of the Euler equations by finite volume methods using Runge-Kutta time stepping schemes. *AIAA Paper 81-1259*, 1981.
36. Aplevich JD. *The Essentials of Linear State-Space Systems*. Wiley: New York, 2000.
37. Doetsch G. *Guide to the Application of the Laplace and Z-transforms* (2nd edn). Van Nostrand Reinhold Company: New York, 1971.
38. McGillem CD, Cooper GR. *Continuous and Discrete Signal and System Analysis*. CBS Publishing Japan Ltd, Japan, 1984.
39. AGARD, *Compendium of Unsteady Aerodynamic Measurements*. AGARD Report No. 702, 1982.
40. Tang D, Kholodar D, Juang J-N, Dowell EH. System identification and proper orthogonal decomposition method applied to unsteady aerodynamics. *AIAA Journal* 2001; **39**(8).
41. Gaitonde AL, Jones DP. *System identification and reduction from the pulse responses of a linearized Euler scheme*. CEAS Aerospace Aerodynamics Research Conference, Cambridge, 2002.

